

Nanopore sequencing as a rapid tool for identification and pathotyping of avian influenza A viruses

Beate M. Crossley,¹  Daniel Rejmanek, John Baroch, James B. Stanton, Kelsey T. Young, Mary Lea Killian, Mia K. Torchetti, Sharon K. Hietala

Abstract. We report whole-genome sequencing of influenza A virus (IAV) with 100% diagnostic sensitivity and results available in <24–48 h using amplicon-based nanopore sequencing technology (MinION) on clinical material from wild waterfowl ($n = 19$), commercial poultry ($n = 4$), and swine ($n = 3$). All 8 gene segments of IAV including those from 14 of the 18 recognized hemagglutinin subtypes and 9 of the 11 neuraminidase subtypes were amplified in their entirety at >500× coverage from each of 16 reference virus isolates evaluated. Subgenomic viral sequences obtained in 3 cases using Sanger sequencing as the reference standard were identical to those obtained when sequenced using the MinION approach. An inter-laboratory comparison demonstrated reproducibility when comparing 2 independent laboratories at ≥99.8% across the entirety of the IAV genomes sequenced.

Key words: avian influenza A virus; MinION; nanopore; whole-genome sequencing.

Introduction

The disease severity seen with different subtypes of influenza A virus (IAV; *Orthomyxoviridae*, *Alphainflenzavirus*) infecting domestic and wild waterfowl is extremely variable, ranging from no clinical disease to situations of extremely high morbidity and mortality.¹⁰ Importantly, the hemagglutinin (H)5 and H7 subtypes of IAV are known to be high risk for severe disease in commercial poultry, and therefore are associated with strict regulatory actions, including depopulation and restricted trade in many countries.³ Given the potential for serious economic consequences, timely and accurate detection are critical for the surveillance and control of IAV in commercial poultry, as well as for wildlife surveillance programs.

The most rapid approach widely utilized for IAV detection is real-time PCR (rtPCR) screening targeting the IAV matrix gene, followed by H5 and H7 rtPCR for those samples testing positive for the IAV matrix gene.¹¹ Official confirmation of positive IAV results is typically performed by the country's national laboratory (e.g., the U.S. Department of Agriculture, National Veterinary Services Laboratories; USDA NVSL). This has historically been conducted by amplicon-based Sanger sequencing from clinical material to determine the hemagglutinin (H or HA) and neuraminidase (N or NA) subtypes and the pathogenicity based on known genetic markers. This process usually requires a minimum of 2 d, depending on the time required for shipping and the virus concentration in the original specimen. Our goal was to evaluate a feasible mechanism for reducing turnaround time

(TAT) to preliminary virus characterization, noting that laboratories that conduct such testing should ensure compliance with their national surveillance and response program(s), and with the Select Agent Program in the United States. Further virus characterization, including virus recovery, whole-genome sequencing (WGS), and intravenous pathogenicity testing, may require weeks, but typically should not impact outbreak response.

We report here rapid and accurate WGS via amplicon-based nanopore nucleic acid sequencing using the MinION system (Oxford Nanopore Technologies; ONT), a commercial portable, real-time device. The MinION system has been shown to be a valid tool for rapid sequencing of RNA and DNA viruses including Ebola virus, infectious laryngotracheitis virus, Zika virus, and salmonid RNA viruses.^{1,4,8,9} Having a segmented genome with nearly identical terminal regions on each segment, IAV is particularly suitable for

California Animal Health and Food Safety Laboratory, University of California–Davis, Davis, CA (Crossley, Rejmanek, Hietala); USDA, Wildlife Services, Fort Collins, CO, retired (Baroch); Department of Pathology College of Veterinary Medicine, University of Georgia, Athens, GA (Stanton, Young); National Veterinary Services Laboratories, Ames, IA (Killian, Torchetti).

¹Corresponding author: Beate M. Crossley, California Animal Health and Food Safety Laboratory, 620 West Health Sciences Drive, University of California–Davis, Davis, CA 95616.
BCrossley@ucdavis.edu

amplicon-based nanopore sequencing given that the entire genome can be amplified using just 3 individual primers.⁵

We evaluated the ability to couple on-site PCR with MinION system WGS in potentially <24 h as a rapid laboratory tool to 1) sequence all 8 IAV gene segments, 2) verify the IAV *H* gene subtype as reported by existing rtPCR assays, 3) determine the IAV *N* subtype, and 4) generate sequence data for analysis of the IAV hemagglutinin cleavage site, a known pathogenicity marker. We performed diagnostic sensitivity studies using clinical samples to assess field use of amplicon-based nanopore sequencing. Additionally, we assessed whether it would be feasible for diagnostic case material (swab samples) to be accurately sequenced directly (e.g., without prior recovery of virus by standard virus isolation efforts).

Materials and methods

Sample preparation, RNA extraction, and cDNA synthesis

Collection of surveillance samples from wild waterfowl was conducted by the U.S. Department of Agriculture (USDA) Wildlife Services. Oropharyngeal and cloacal swabs were obtained from hunter-collected carcasses and pooled by individual bird ($n = 24$). We used oropharyngeal swabs from 1 commercial chicken and 3 turkeys, and tracheal swab samples from 3 swine, obtained from diagnostic and routine surveillance samples submitted to the California Animal Health and Food Safety Laboratory (CAHFS). All samples were processed and analyzed at the CAHFS Davis laboratory. Viral RNA was extracted from the swab fluid (MagMAX-96 viral RNA isolation kit, KingFisher 96 automated magnetic particle processor; Thermo Fisher) per the manufacturer's instructions, using an elution volume of 90 μ L. Swine lung tissue samples were homogenized (MagNA Lyser; Roche). Briefly, 250 mg of tissue was placed in a 2-mL polypropylene tube containing 1.5 mL of denaturation solution (Ambion) and filled one-quarter full with 2.3-mm silica beads (Bio-Spec Products, Cole-Parmer). The samples were homogenized at 6,500 rpm for 45 s, then incubated at room temperature for 5 min. Next, 20 μ L of proteinase K (20 mg/mL) was mixed with 20 μ L of homogenate and incubated at 56°C for 60 min. The digest was then transferred to a plate (MagMax 96 Express; Thermo Fisher) with 20 μ L of binding beads and 100 μ L of lysis solution per sample. The plate was transferred to a magnetic processor (BioSprint; Qiagen), and RNA extraction was performed (MagMAX-96 viral RNA isolation kit).

Avian IAV RT-rtPCR

A one-step multiplex reverse-transcription rtPCR (RT-rtPCR; VetMAX Gold AIV or SIV detection kit; Thermo Fisher), designed to target viral matrix and nucleoprotein genes, was

used to amplify IAV RNA. The PCR reaction was set up in a 25- μ L volume containing 12.5 μ L of 2 \times multiplex RT-rtPCR buffer, 1.0 μ L of nuclease-free water, 1.0 μ L of IAV primer-probe mix, 2.5 μ L of multiplex RT-rtPCR enzyme mix, and 8.0 μ L of RNA template or controls. A low pathogenicity IAV isolate [A/Turkey/WI/68 (H5N9)] obtained from the USDA NVSL was used as a positive extraction and rtPCR assay control. Nuclease-free water was used as a negative control. The thermocycling reactions were performed (7500 Fast PCR system; Applied Biosystems) under the following conditions: reverse transcription at 48°C for 10 min, reverse transcriptase inactivation/initial denaturation at 95°C for 10 min, and 40 cycles of amplification and extension (95°C for 15 s and 60°C for 45 s).

Influenza PCR and Sanger sequencing

Initially, chicken egg-propagated, high-titer IAV samples ($n = 16$) representing subtypes H1–H12, H14, and N1–N9 isolated from wild waterfowl (green-winged teal, *Anas carolinensis*; mallard, *A. platyrhynchos*; American wigeon, *Mareca americana*; northern shoveler, *A. clypeata*) were prepared for MinION sequencing (Table 1).

Subsequently, wild waterfowl swab samples (same species as above, and northern pintail *A. acuta*; cinnamon teal, *A. cyanoptera*; ring-necked duck, *Aythya collaris*) covering the diagnostic range of cycle threshold (Ct) values (24–36), as well as the diagnostic samples including turkey, chicken, and swine swabs (Ct 19–32) were sequenced directly (no prior virus isolation; Table 2).

In preparation for WGS, the 8 IAV gene segments were amplified simultaneously in a single reaction using an RT-rtPCR with the following universal primers: MBTuni-12 (0.1 μ M), MBTuni-12.4 (0.1 μ M), and MBTuni-13 (0.2 μ M; Table 3).

A 25- μ L reaction was used (Invitrogen Superscript III one-step RT-PCR system, Platinum Taq DNA polymerase high fidelity; Thermo Fisher) and the following thermocycling reactions: 60 min at 42°C, 2 min at 94°C, then 5 cycles of 30 s at 94°C, 30 s at 44°C, 3 min at 68°C, followed by 31 cycles of 30 s at 94°C, 30 s at 57°C, 3 min at 68°C, with a final extension at 68°C for 7 min. For the dilution series experiment, the number of thermocycling reactions was increased from 31 to 40 for a subset of the replicates to ensure analytic sensitivity in the experiment (Table 4).

The same one-step RT-PCR system and thermocycling conditions (31 cycles) were used to reverse transcribe and amplify all genome segments, individually, from 3 different IAV subtypes (H1N1, H3N8, and H8N4) using segment-specific primers (Table 3). PCR amplicons were visualized by agarose gel electrophoresis, followed by purification using a 1:1 ratio of AMPure XP beads (Beckman Coulter). IAV

Table 1. Diversity of avian influenza A virus subtypes used for MinION sequencing.

| Subtype | Host | Sample ID | GenBank accessions |
|---------|-------------------|-----------|--------------------|
| H1N1 | Green-winged teal | AH0092236 | MK905364–371 |
| H2N3 | Mallard | AH0025218 | MK928172–179 |
| H3N2 | American wigeon | AH0115661 | MK928140–147 |
| H3N8 | Mallard | AH0033218 | MK928188–195 |
| H4N6 | Mallard | AH0101955 | MK928180–187 |
| H5N2 | Green-winged teal | AH0047889 | MK928156–816 |
| H6N5 | American wigeon | AH0025977 | MK928132–139 |
| H7N8 | Mallard | AH0115568 | MK928212–219 |
| H8N4 | Northern shoveler | AH0079885 | MK928220–227 |
| H9N2 | Mallard | AH0033695 | MK928196–203 |
| H10N3 | Green-winged teal | AH0093155 | MK928148–155 |
| H10N7 | Green-winged teal | AH0115705 | MK928164–171 |
| H10N9 | Northern shoveler | AH0087956 | MK928244–251 |
| H11N2 | Mallard | AH0115668 | MK928204–211 |
| H12N2 | Northern shoveler | AH0047767 | MK928236–243 |
| H14N3 | Northern shoveler | AH0093075 | MK928228–235 |

Table 2. Details of influenza A viruses sequenced in our study.

| Host | Sample ID | Ct | Subtype(s) | GenBank accessions |
|-------------------|-----------|----|------------------------|--------------------|
| American wigeon | AH0138185 | 28 | H6N1 | MK995694–701 |
| Cinnamon teal | AH0093291 | 29 | H4, H6, H12 N2, N5 | MK995710–727 |
| | AH0093904 | 35 | H6N2 | MK995702–710 |
| | AH0138496 | 29 | H7N3 | MK995728–735 |
| Green-winged teal | AH0094001 | 27 | H7, H11 N3, N9 | MK995744–759 |
| | AH0137747 | 36 | Incomplete genome | |
| | AH0137989 | 27 | H11N2 | MK995736–743 |
| | AH0138674 | 27 | H5, H9, H11N9 | MK995760–776 |
| | AH0152086 | 35 | Incomplete genome | |
| Mallard | AH0158391 | 31 | H9N2 | MK995777–784 |
| | AH0092950 | 35 | H11N9 | MK995785–792 |
| | AH0093042 | 34 | H9N2 | MK995793–800 |
| | AH0121061 | 34 | H12N5 | MK995801–808 |
| | AH0152465 | 26 | H5N2 | MK995809–816 |
| Northern pintail | AH0152537 | 27 | H10N3 | MK995817–824 |
| | AH0137555 | 29 | H12N2 | MK995825–832 |
| | AH0137836 | 35 | Incomplete genome | |
| Northern shoveler | AH0093889 | 34 | H9N2 Incomplete genome | |
| | AH0093952 | 24 | H8N4 | MK995833–840 |
| | AH0138031 | 24 | H1N1 | MK995841–848 |
| | AH0138661 | 30 | H7 N3, N9 | MK995849–857 |
| | AH0138715 | 34 | H5N3 Incomplete genome | |
| Ring-necked duck | AH0152245 | 32 | H5N2 | MK995858–865 |
| | AH0137654 | 28 | H5N2 | MK995866–873 |
| Chicken | B1801923 | 24 | H7N3 | MN179383–390 |
| Swine | T1800664 | 32 | H1N1 | MN179391–398 |
| | T1801615 | 24 | H1N2 | MN179399–406 |
| | T1801856 | 28 | H1N2 | MN179407–414 |
| Turkey | B1801739 | 19 | H7N3 | MN179359–366 |
| | B1801783 | 24 | H7N3 | MN179367–374 |
| | B1801968 | 25 | H7N3 | MN179375–382 |

Ct = influenza A virus quantitative PCR cycle threshold values. Incomplete genomes included the following segments: AH0137747 (NS, M, PB2); AH0137836 (NS); AH0152086 (PB1); AH0093889 (HA, NA, M, NS, PA); AH013871 (HA, NA, M, NS, PA).

Table 3. Oligonucleotide primers used in our study.

| Primer | Oligonucleotide sequence (5'–3') | Reference |
|-------------------------|----------------------------------|----------------------------------|
| Universal primer | | |
| MBTuni-12 | ACGCGTGATCAGCAAAAAGCAGG | Zhou and Wentworth ¹² |
| MBTuni-12.4 | ACGCGTGATCAGCGAAAAGCAGG | Zhou and Wentworth ¹² |
| MBTuni-13 | ACGCGTGATCAGTAGAAAACAAGG | Zhou and Wentworth ¹² |
| Segment-specific primer | | |
| PB2-F | TATTGGTCTCAGGGAGCGAAAAGCAGGTC | Hoffmann et al. ⁵ |
| PB1-F | TATTCGTCTCAGGGAGCGAAAAGCAGGCA | Hoffmann et al. ⁵ |
| PA-F | TATTCGTCTCAGGGAGCGAAAAGCAGGTAC | Hoffmann et al. ⁵ |
| HA-F | TATTCGTCTCAGGGAGCAAAAAGCAGGGG | Hoffmann et al. ⁵ |
| NP-F | TATTCGTCTCAGGGAGCAAAAAGCAGGGTA | Hoffmann et al. ⁵ |
| NA-F | TATTGGTCTCAGGGAGCAAAAAGCAGGAGT | Hoffmann et al. ⁵ |
| M-F | TATTCGTCTCAGGGAGCAAAAAGCAGGTAG | Hoffmann et al. ⁵ |
| NS-F | TATTCGTCTCAGGGAGCAAAAAGCAGGGTG | Hoffmann et al. ⁵ |
| PB2-int-R | TGTAGACACTGCTTGTCCACCAGC | Current study |
| PB1-int-R | CCTCTGATTTGCATTCCGGGTGT | Current study |
| PA-int-R | CTGGAGAAGTTCGGTGGGAGACTT | Current study |
| HA-H1N1-R | TGTTGTTCACCTGGTGGTCCGAGGAT | Current study |
| HA-H3N8-R | CTGGTTTGTGCTTGGATGATGAACTCC | Current study |
| HA-H8N4-R | TCCTTGTGTCTCTGACCAATGGTC | Current study |
| NP-int-R | TCCGATCATTGATCCCTCGCTTGATC | Current study |
| NA-H1N1-R | CATTGTCTGGGCCGAAATACCAATTG | Current study |
| NA-H3N8-R | CCACTGCTACTGCTTTGGCATCAGG | Current study |
| NA-H8N4-R | CATCCTGGCATAACGACTCGGAC | Current study |
| M-int-R | GACCAGCACTGGAGCTAGGATGAGTCC | Current study |
| NS-int-R | GTGGAGGTCTCCCATCTCATTACTGC | Current study |

Table 4. Dilution series showing detection and coverage of influenza A virus H3N8 segments following MinION sequencing.

| Dilution | PCR cycles | NS | M | NA | NP | HA | PA | PB1 | PB2 |
|-------------|------------|------|------|------|------|---------|------|------|--------|
| Neg Control | 40 | ND | ND | ND | ND | ND | ND | ND | ND |
| Ct-32 | 31 | High | High | High | High | High | High | High | High |
| Ct-35 | 31 | High | High | High | High | High | Med | High | High |
| Ct-35 Rep 1 | 40 | High | High | High | High | High | High | High | High |
| Ct-35 Rep 2 | 40 | High | High | High | High | High | Med | High | High |
| Ct-35 Rep 3 | 40 | High | High | High | High | High | High | High | High |
| Ct-38 Rep 1 | 31 | Low | Low | ND | ND | Low | ND | ND | ND |
| Ct-38 Rep 2 | 31 | ND | ND | ND | Low | Low | Low | ND | ND |
| Ct-38 Rep 3 | 31 | High | ND | Med | Low | High-IS | ND | Low | Low |
| Ct-38 Rep 1 | 40 | High | High | ND | ND | High-IS | High | Med | Med |
| Ct-38 Rep 2 | 40 | ND | High | High | High | ND | ND | ND | Low-IS |
| Ct-38 Rep 3 | 40 | ND | ND | High | ND | ND | ND | ND | Low |
| Ct-41 | 31 | ND | ND | ND | ND | ND | ND | ND | ND |
| Ct-41 Rep 1 | 40 | ND | ND | ND | ND | ND | ND | ND | ND |
| Ct-41 Rep 2 | 40 | ND | ND | Low | ND | ND | ND | ND | ND |
| Ct-41 Rep 3 | 40 | ND | Med | ND | ND | ND | ND | ND | Low-IS |

Dilutions indicate influenza A virus matrix gene quantitative PCR cycle threshold (Ct) values and number of replicate MinION sequencing runs. The coverage of each gene segment is indicated as High (>200×), Medium (Med; 50–200×), or Low (<50×). IS = incomplete segment sequenced; ND = no detection.

segment amplicons were sequenced using Sanger sequencing (ELIM Biopharmaceuticals). A final contiguous sequence for each segment was generated by aligning forward and reverse sequences using the program Geneious Prime v.2019.0.4 (Biomatters).

Library preparation and WGS

For DNA library preparation, 1 µg of purified universal PCR amplicon from each sample was the input to a library generated with the Ligation sequencing kit 1D SQK-LSK108 (ONT). First, DNA was end-repaired (NEBNext Ultra II end repair/dA tailing kit; New England Biolabs), purified using AMPure XP beads in a ratio of 1:1 volume of beads per sample, and eluted in 30 µL of nuclease-free water. Sequencing adapters (AMX1D; ONT) were ligated to the DNA (Blunt/TA ligation master mix; New England Biolabs) by incubation at room temperature for 10 min. The adapter-ligated DNA library was purified with AMPure XP beads in a ratio of 1:2.5 volume of beads per sample, followed by 2 washes (Adapter bead binding buffer; ONT) and elution in 15 µL of elution buffer (ONT). The library was loaded onto a MinION flowcell (MIN106 R9.4; ONT) and run via MinKNOW v.18.05.5 for up to 48 h. MinKNOW-generated FASTQ files containing 4,000 “pass” reads (Q score ≥ 7) per file were loaded into Geneious Prime, and were initially mapped to a set of reference IAV genome segments from wild birds in the United States within the past 10 y (GenBank H1: KY284523; H2: MH637361; H3: KY828741; H4: CY235331; H5: MH546211; H6: KY983185; H7: KR077940; H8: CY034159; H9: KY983229; H10: MG280432; H11: KX351573; H12: KY563737; H13: CY070874; H14: KX024583; N1: MG280254; N2: KY990792; N3: KU289945; N4: KY983212; N5: KY983191; N6: MN253938; N7: CY186774; N8: MN253966; N9: KY990784; M: KY983210; NS: KY990767; NP: KY561074; PA: MK928193; PB1: MH251192; PB2: KY983147).

For most samples, the number of reads generated far exceeded the amount needed to generate high coverage ($>500\times$) consensus sequences. Hence, only a fraction of all files was mapped to each reference segment. In order to achieve $500\times$ coverage across each entire segment, 500–1,000 mapped reads needed to be generated. Depending on the segment (shorter segments were more abundant) mapping of 5–40 files from an average of 500 files was sufficient to achieve 1,000 mapped reads. The resulting consensus sequences were compared to GenBank using BLASTn (<http://www.ncbi.nlm.nih.gov/blast/Blast.cgi>). The “top hit” was then used as a reference sequence for a second round of read mapping. Mapping was set at 5 iterations and a 65% consensus threshold.

Final consensus sequences were manually inspected for any single-base ambiguities, which are known to be possible at longer homopolymer regions (i.e., AAAAA).⁶ This manual step was included to ensure that a consensus sequence

containing an ambiguous base (usually an “N”) in the homopolymer region did not occur as a result of the detection algorithm incorrectly accounting for all of the bases in these homopolymer regions. In such cases, the ambiguous base was manually replaced with the base detected most commonly by visual identification at that site among all aligned sequences. Primer sequences were manually trimmed, and final consensus sequences from all unique samples with a minimum $100\times$ depth of coverage across the entire segment were submitted to GenBank.

Analytic sensitivity testing

An avian-origin H3N8 IAV isolate was used to establish the analytic sensitivity of the MinION sequencer for recovering IAV genome data following universal IAV RT-rtPCR amplification. To mimic the same sample matrix used for standard diagnostic sampling, a high-titer H3N8 isolate (low Ct value) was serially diluted 10-fold in pooled viral transport medium (VTM) obtained from IAV-negative oropharyngeal and/or cloacal waterfowl swabs previously submitted to CAHFS for testing. Preliminary testing verified these spiked dilutions, as tested by RT-rtPCR, to have Cts spanning the limit of detection of MinION sequencing (Ct 32, 35, 38, and 41). The Ct 35, 38, and 41 dilutions were PCR amplified and sequenced in triplicate. In an effort to maximize analytic sensitivity during the experiments, the number of PCR cycles was increased from 31 to 40 for several of the dilutions tested. A negative control consisting of IAV-negative VTM was included as part of the analytic sensitivity experiment.

Diagnostic sensitivity and specificity

We assessed MinION-based IAV WGS for feasibility of use as a tool for detection of naturally occurring IAV infections in routine clinical and surveillance samples. Twenty-four wild waterfowl samples obtained from 7 different species with a range of rtPCR Ct values were amplified and sequenced. In addition, 1 chicken and 3 turkey samples obtained during an autumn 2018 outbreak of low pathogenicity avian influenza (LPAI) were tested. Lastly, samples obtained from 3 pigs testing positive previously for IAV were included in the validation assessment. The identity of the IAV, including N subtype, H subtype, and existence or absence of known pathogenicity markers at the cleavage site of H5 and H7 subtypes,⁷ were confirmed by comparison of the whole-genome sequences obtained during the testing to IAV whole virus reference genomes, including LPAI and highly pathogenic avian influenza strains, found in GenBank.

Inter-laboratory reproducibility

To demonstrate inter-laboratory reproducibility of the MinION-based IAV WGS results generated at CAHFS, RNA

extracts from 10 unique IAV subtypes were sent on dry ice to a laboratory at the University of Georgia (UGA; Athens, GA) with prior MinION sequencing experience. The UGA laboratory was provided with the protocols and primers used at CAHFS. Sequences were analyzed similarly to the methods described above, with the differences as follows. Base calling was conducted using Albacore v.2.3.4 (ONT), and adapter sequences were trimmed using Porechop v.0.2.3 (<https://github.com/rrwick/Porechop>). To sort the reads based on avian IAV (AIV) segments, sequences were initially mapped, without iterations, to a file containing one sequence for each AIV HA and NA segment. The top hit was then used as a reference sequence for a second round of read mapping. The remaining non-HA and non-NA reads were identified and sorted by mapping and consensus building to the non-HA and non-NA segments of a single AIV isolate. The ends of short reads caused by mispriming were trimmed to remove erroneous, primer-based sequences. Consensus sequence threshold was set to “0% majority,” and single-nucleotide deletions or insertions at homopolymers were subsequently corrected manually to remove frameshifts. All mapping and consensus building were performed using Geneious Prime v.2019.0.4. Primer sequences were trimmed from the end of the consensus sequences, and consensus sequences were then compared between the 2 laboratories.

Results

IAV diversity using cultured IAV

To evaluate the utility of the MinION-based WGS approach for detecting a diversity of IAV subtypes, we sequenced 16 isolates encompassing 13 of the 18 recognized HA types and 9 of the 11 recognized NA types (Table 1). The only types not available for testing were the bird-associated H13, H15, and H16 subtypes, and the bat-associated subtypes H17N10 and H18N11. All 8 segments in their entirety were amplified at a minimum 500× depth of coverage from each of the 16 isolates.

Comparison of MinION to Sanger sequencing

To validate the accuracy of IAV sequencing using the amplicon-based nanopore sequencing (i.e., the MinION-WGS approach) compared to the industry-standard Sanger sequencing, internal sequences from all 8 segments from 3 IAV isolates (H1N1, H3N8, and H8N4) were sequenced by the Sanger method and sequence results were compared with the MinION-generated consensus sequences from the same isolates. The sequences ranged in length from 622 bp (NA, H1N1) to 774 bp (PB-1, H8N4). For the 3 isolates analyzed, sequences generated using the Sanger method were identical to the MinION-generated consensus sequences across all 8 segments (i.e., 24 total sequences).

Analytic sensitivity

The analytic sensitivity was determined by serial dilution of a previously characterized H3N8 isolate sequenced using MinION WGS following universal IAV RT-rtPCR (Table 4). The dilution series was designed to include a range of matrix gene rtPCR Ct values that encompassed the limit of detection for MinION sequencing. The Ct values obtained ranged from a low of Ct 32, for which all segments of the virus were sequenced at high coverage depth (>200×), to Ct 41, for which only a few segments were detected at low (<50×) or medium (50–200×) coverage depth in 2 of 3 replicates after 40 PCR cycles. Based on these data, a limit of detection rtPCR Ct value of 35 was determined as appropriate to ensure that all segments are detected consistently with high coverage. Additionally, increasing the number of PCR cycles from 31 to 40, as evaluated in the dilution series, demonstrated that individual segments from the 40-cycle group were detected at a higher depth of coverage compared to the 31-cycle group. However, the total number of segments detected (at any depth of coverage) was nearly identical between the 2 groups.

Diagnostic sensitivity and specificity

Among the wild waterfowl samples, complete genomes were recovered for all samples with Ct values of 32 or below (Table 2). Although 4 complete genomes were recovered from 9 samples with Ct values of 34 and 35, the other 5 samples resulted in at least partial genome coverage. Of the 19 waterfowl samples for which complete genomes were recovered, 4 had mixed IAV infections and, in 2 of those, 3 different HA subtypes were detected. From the 4 poultry samples (1 chicken, 3 turkeys), nearly identical H7N3 genomes were recovered. None of the 5 waterfowl H5 or H7 subtypes, nor the 4 poultry H7 subtypes evaluated, contained known pathogenicity markers at the HA cleavage site.

Inter-laboratory reproducibility

Sequence comparisons were made using consensus sequences following manual editing of single-nucleotide deletions or insertions at homopolymers (Table 5). The sequence identities between CAHFS and UGA were nearly identical. Three of the 80 segments compared were 99.8% identical, 17 were 99.9% identical, and 60 were 100% identical.

Turnaround time

Considering all of the steps involved in MinION system WGS, we evaluated an approximate TAT from swab to genome data for an IAV sample. The initial RNA extraction procedure from an oropharyngeal swab required ~1 h. Preparing master mix and completing the RT-rtPCR required an additional 2 h. The universal RT-rtPCR, including master mix

Table 5. Percent identity of MinION-generated influenza A virus sequences between CAHFS and the University of Georgia.

| Segment | Subtype | | | | | | | | | |
|---------|---------|------|------|------|-------|-------|-------|-------|------|------|
| | H1N1 | H4N6 | H7N8 | H8N4 | H10N3 | H10N7 | H11N2 | H14N3 | H5N2 | H3N2 |
| HA | 100 | 100 | 100 | 100 | 100 | 99.8 | 100 | 100 | 99.8 | 99.9 |
| NA | 100 | 100 | 100 | 100 | 99.9 | 100 | 99.9 | 100 | 100 | 99.9 |
| PB2 | 100 | 100 | 100 | 100 | 100 | 100 | 100 | 99.9 | 100 | 99.9 |
| PB1 | 100 | 99.9 | 99.9 | 100 | 100 | 100 | 100 | 99.9 | 100 | 99.9 |
| PA | 100 | 100 | 99.9 | 100 | 100 | 99.9 | 100 | 99.9 | 100 | 99.9 |
| NS | 100 | 100 | 100 | 100 | 100 | 100 | 99.8 | 100 | 100 | 100 |
| NP | 100 | 100 | 99.9 | 100 | 100 | 100 | 99.9 | 100 | 100 | 99.9 |
| M | 100 | 100 | 100 | 100 | 100 | 100 | 100 | 100 | 100 | 100 |

preparation, required ~4 h. The MinION DNA library preparation required an additional 3 h to complete prior to placing the sample on a flowcell for sequencing. Because data generated by the MinION is available for analysis in real time, subtyping was possible in as little as 1 h after starting the MinION sequencing run for nearly all of the samples tested (e.g., those with RT-PCR Cts <32). Finally, complete post-sequence data analysis required, on average, an additional 4 h. Thus, a minimum of 15 h was needed from the time a swab sample having a sufficient concentration of virus arrived in the laboratory to the availability of a complete IAV genome.

Discussion

We demonstrated the feasibility of generating whole-genome sequence data direct from clinical samples within 1–2 days on-site. Rapid TATs and completeness of the laboratory results can be critical where morbidity and mortality are high in poultry or when there is human involvement (e.g., reverse zoonosis from humans to pigs). The use of the MinION-WGS approach described here can reduce the time from submission of a swab sample to IAV subtype in a positive sample to as little as a single day. For the purpose of our study, an extended MinION sequencing run time of 48 h was used; however, the clinical samples with lower initial Ct values (e.g., Cts <32, which equates to higher virus concentration) had sufficient sequence data for quality evaluation after as little as 1 h of sequence time. For example, from sample AH0152245, which had a quantitative PCR Ct of 32, 176,000 reads passing internal quality parameters (Q score ≥ 7) were generated within 1 h of sequencing. Of those sequences, 53,000 mapped variably to each of the 8 IAV segments ranging from 1,600 reads (PB2) to 18,200 reads (NS) resulting in high coverage consensus sequences covering the entire genome. Because the MinION system allows access to data during the sequencing process, the data can be reviewed and analyzed in real-time thus shortening the actual run time and associated TAT to the result.

Use of WGS via the MinION system allows for on-site and rapid generation of diagnostic quality data for IAV to determine the H and N subtypes and presence of known

pathogenicity markers. Additionally, sequence data can be uploaded via designated portals to reference laboratories or collaborating laboratories for analysis and assessment when concerns regarding zoonotic potential or altered pathogenicity exist. However, our study highlights the need to manually inspect consensus sequences for long homopolymer regions, as well as any associated single-base ambiguities. The next generation of flowcells (v.R10) contains engineered nanopores with additional recognition sites to better resolve homopolymer regions, thus, in the future minimizing the problems detected with homopolymers. The real-time availability of MinION system sequencing data is useful for disease investigations, as well as routine surveillance. Real-time virus monitoring could also be useful when poultry are held and allowed to clear LPAI prior to marketing.

Wild waterfowl samples were specifically targeted in the diagnostic laboratory setting to verify the MinION system given the potential presence of PCR inhibitors in the sample matrix.² Additionally, swab samples from commercial poultry, as well as a small subset of swine samples were evaluated using the MinION system. The IAV obtained from 4 commercial poultry samples (1 chicken, 3 turkeys) from the same H7N3 LPAI outbreak were sequenced and found to be nearly identical.

We compared the MinION system WGS to viral genome sequences obtained by Sanger sequencing across large sections (622–774 bp) of all 8 segments from 3 different IAV subtypes. The MinION data reliably generated whole genomes direct from swab samples without the need for prior isolation of the virus, as can be done with Sanger sequencing; however, the ability to generate data across the full genome can save valuable time in support of outbreak or disease investigation responses. Our data using serial dilutions of known IAV suggest that samples with a PCR Ct ≤ 35 are appropriate for attempted sequencing by the MinION system; whereas Cts <32 are more likely to yield acceptable data across all 8 segments of the virus (>200 \times). Our study highlights the feasibility and benefits of nanopore sequencing using a bench-top MinION system that can provide near real-time access to high-quality whole-genome IAV data

direct from clinical material, as well as IAV isolates. This approach could be expanded to include a subset of other infectious agents, dependent on size and complexity of the genome, as a reasonable on-site option for diagnostic laboratories given the accessibility, affordability, and portability of the MinION system.

Acknowledgments

We acknowledge the programs that supported sample collection: the U.S. Interagency Wild Bird Surveillance program, the National Poultry Improvement Program, and the USDA Swine Surveillance program.


Declaration of conflicting interests

The authors declared no potential conflicts of interest with respect to the research, authorship and/or publication of this article.

Funding

Financial support for studies performed at the California Animal Health and Food Safety Laboratory were provided by California Food and Agricultural Code Section 224 (f)(1) funding awarded by the California Department of Food and Agriculture. The University of Georgia analysis was supported by Agriculture and Food Research Initiative Competitive Grant 2018-67015-28306 from the USDA National Institute of Food and Agriculture.

ORCID iD

Beate M. Crossley  <https://orcid.org/0000-0003-2932-7229>

References

1. Das A, et al. Removal of real-time reverse transcription polymerase chain reaction (RT-PCR) inhibitors associated with cloacal swab samples and tissues for improved diagnosis of avian influenza virus by RT-PCR. *J Vet Diagn Invest* 2018;21:771–778.
2. Gallagher MD, et al. Nanopore sequencing for rapid diagnostics of salmonid RNA viruses. *Sci Rep* 2018;8:16307.
3. Halvorson DA. The control of H5 or H7 mildly pathogenic avian influenza: a role for inactivated vaccine. *Avian Pathol* 2002;31:5–12.
4. Hoenen T, et al. Nanopore sequencing as a rapidly deployable Ebola outbreak tool. *Emerg Infect Dis* 2016;22:331–334.
5. Hoffmann E, et al. Universal primer set for the full-length amplification of all influenza A viruses. *Arch Virol* 2001;146:2275–2289.
6. Rang FJ, et al. From squiggle to basepair: computational approaches for improving nanopore sequencing read accuracy. *Genome Biol* 2018;19:90.
7. Senne DA, et al. Survey of the hemagglutinin (HA) cleavage site sequence of H5 and H7 avian influenza viruses: amino acid sequence at the HA cleavage site as a marker of pathogenicity potential. *Avian Dis* 1996;40:425–437.
8. Spatz SJ, et al. MinION sequencing to genotype US strains of infectious laryngotracheitis virus. *Avian Pathol* 2019;48:255–269.
9. Quick J, et al. Multiplex PCR method for MinION and Illumina sequencing of Zika and other virus genomes directly from clinical samples. *Nat Protoc* 2017;12:1261–1276.
10. Verhagen JH, et al. Ecology and evolution of avian influenza viruses. In: Tibayrenc M, ed. *Genetics and Evolution of Infectious Disease*. Elsevier, 2011:729–749.
11. World Organisation for Animal Health (OIE). Avian influenza (infection with avian influenza viruses), Chapter 3.3.4. In: *Terrestrial Manual*. OIE, 2018. [cited 2020 Jan 10]. https://www.oie.int/fileadmin/Home/eng/Health_standards/tahm/3.03.04_AI.pdf
12. Zhou B, Wentworth DE. Influenza A virus molecular virology techniques. In: Kawaoka Y, Neumann G, eds. *Influenza Virus: Methods and Protocols*. Vol. 865, *Methods in Molecular Biology*. Humana Press, 2012:175–191.